Journal of Hydraulic Structures
J. Hydraul. Struct., 2024; 10(3): 18-33
DOI: 10.22055/jhs.2024.44714.1263

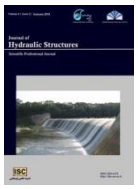

OPEN ACCESS

Experimental study of contaminant mixing through the buried river junctions

Jafar Chabokpour[1]

Abstract

Rivers, as water resources, are considered an origin of supply for many requirements of urban communities. River networks consist of many branches that connect at river confluences. Because pollutants usually enter the river in different situations from the upstream branches of river intersections, it is essential to investigate the mixing process through the river network. For this purpose, precise analytical and numerical models should be used to evaluate this phenomenon quantitatively. Based on the cell concept and separation of advection and dispersion operations, this study developed a new analytical relationship through the confluences of rivers. A physical model of the Y-shaped junction was created in the laboratory, and four inlet flow discharges 25, 21, 12, and 9 l/s and three initial concentrations of sodium chloride solution 80, 160, and 200 g/L were selected as study parameters. Then, the concentration-time curves along the sub-branches, the intersection, and the downstream of the river's main channel were taken at 2-second intervals. In order to evaluate the efficiency of the analytical model, the parameters of the model were first calculated by coding based on its framework and using the least squares method. Then the analytical curves were outlined versus the experimental results. It was observed that the presented model could produce double-peaked curves and also cover experimental data series precisely. The dispersion coefficients and the related time parameter in the presented model (T) were found to increase by moving downstream of the river junction. It was also observed that the Peclet numbers ($P_e = \frac{xu}{D}$) are increased like dispersion coefficients by increasing the distance downstream of the confluence. In addition, the research results showed that increasing the residence time parameter in dispersion cells (T) causes growth in the dispersion coefficient, despite increasing the residence time in advection cells (β), compelling the movement of the pollutant breakthrough curves.

Keywords: Pollutant, river junction, breakthrough curve, mixing, analytical model.

Received: 04 September 2023; Accepted: 31 March 2024

1. Introduction

The importance of solute transport in streams extends beyond aquatic ecosystems. Streams are a significant source of freshwater for human consumption, agriculture, and industry. Therefore, understanding how solutes move through stream networks is crucial for water resource

[1] civil engineering department, University of Maragheh, Maragheh, Iran, Email: J.chabokpour@maragheh.ac.ir **(Corresponding author)**

management. Monitoring the quality and concentration of solutes, particularly those related to human activities, can help ensure the safety and sustainability of our water supply [1, 2].

River networks are one of the types of aquatic ecosystems. In these networks, different river branches are connected through river junctions. Exploration regarding hydraulics and flow structure in different types of river intersections has been discussed for a long time. The current patterns through the confluences cause morphological changes and affect the pollution-spreading processes in rivers. The flow ratios of different branches, the angle of river branches concerning each other, and the characteristics of river bed materials are essential and influential parameters in the mixing mechanism [3-6]. Previous studies have focused more on the flow structure and the factors affecting it. Best has done the most fundamental investigation in this field. In his study, six general flow structures were identified in river junctions. Also, the discharge ratio and the angle of the branches introduced essential parameters affecting the flow pattern [3-7].

Solute transport in streams is a complex process influenced by several factors, including hydrological conditions, geological features, and human activities. One of the primary mechanisms of solute transport in streams is advection. Advection refers to the physical movement of solutes with the flowing water. As water travels downstream, solutes dissolved in it move along, creating a downstream gradient. The rate of advection depends on the velocity of the water, and different solutes may have varying speeds of transport. Another important mechanism is hydrodynamic dispersion, which is sum of mechanical dispersion (due to turbulence and mixing) and molecular dispersion and involves the spreading of solutes in the water due to turbulence and mixing. This process occurs because the velocity of water is not uniform across a stream cross-section. Dispersion helps distribute solutes evenly, preventing localized spikes in concentration. Consequently, it supports a more stable and balanced aquatic ecosystem. Additionally, biochemical processes occurring in the stream can influence solute transport. For example, biological uptake involves the absorption of solutes by stream organisms such as algae, bacteria, and other plants. The uptake of nutrients like phosphates or nitrates is beneficial, as it helps regulate their concentration. However, excessive nutrient uptake could lead to imbalances and negatively affect aquatic life [8, 9].

Best & Reid [7] found that with the increase in the discharge ratios, the length and width of the separation zone in river junctions improved, but its shape index (the ratio of maximum width to length) remained constant. Qing-Yuan et al. [10] found that the isoline method, in which the boundary of the separation zone is determined using the zero longitudinal velocity line, is more accurate than the streamline method. In addition to the mentioned cases, transverse eddies and their advection downstream have been proven at the river junction. The presence of these vortices increases the stress and, as a result, erosion at the intersection, which ultimately causes morphological changes in the intersection [4, 11].

Through high-frequency velocimeter devices, Biron et al. [12] and Rhoads & Sukhodolov [13] acquired the velocity data through the natural river junctions and studied the shear layer in the intersection. Shakibainia et al. [14] reported the existence of three types of swirling currents in the main channel, the branch, and the separation zone. They claimed that the eddy currents in the separation zone are the primary causality for forming the separation zone. They also claimed that this type of swirling currents did not exist at the intersections of natural rivers due to sedimentation, while the swirling currents formed by the sub-branches were due to the deviation of the general flow path. Through the junction, it is the most vital type of swirling current, and the interference with the swirling flow of the branch also causes the swirling flow related to the main channel. The swirling currents related to the main river channel also become more assertive and

more dominant with the increase in the angle of the sub-channel and the ratio of discharges [14, 15].

Many researchers have widely studied the effect of the 3D structure of river junctions' location on the intersection's hydrodynamics. The flow deviation in the river's main channel may not exist due to the three-dimensional conditions of the bed at the intersection, and as a result, the separation zone is diverted to zones with lower depths. In this case, the separation region is apparent at the surface of the flow, but this zone will not exist at the lower flow depths [16-19].

Many studies on hydrodynamic characteristics through the river junctions have been done; however, sufficient studies have not been conducted on the mixing of pollution through the river confluences. The operated investigations are mainly based on the mixing rate. Based on the research done by [20] , deep mixing is achieved in length equal to several tens of times the average flow depth, but completing transverse mixing requires a much longer length. They claimed that for a wide river, the required length for complete transverse mixing is 100-1000 times the main channel width. However, other researchers such as Gaudet & Roy [21] reported this mixing much faster and claimed that this mixing is completed at a distance equal to 25 times the river channel width. Both previous experimental and numerical studies have increased our knowledge about the flow structure and the mixing process, but most of the experimental data, due to the limitations of the measurement tools, are not accurate for predicting the complex mechanism of mixing through the confluences. For this reason, numerical modeling has been used as a complementary tool to experimental analysis. Mignot et al. [22] used the turbulence (k-ϵ) model to simulate the applied lateral flow.

Also, many previous studies have been done on irregular junction shapes, which causes an uncertainty in results. There are also regular types of river intersections, named Y-shaped confluence, in which their analysis results are more comprehensive.

Weidong et al.; Weidong & Yue [23, 24] studied the flow patterns using the ADV velocimeter data collected through the river confluence. Several zones, named stagnant zone, flow deviation zone, flow separation zone, and acceleration zone, have been observed through the confluences. Also, the circular flow pattern downstream of the junction was observed. Furthermore, with the increase in the flow ratio of the branches, the strength of the rotating current downstream of the junction decreases. Rhoads & Sukhodolov [25] found that the rotational flow downstream of the conjunction increases the mixing rate of passing pollutants. Also, they claimed that in regular geometric confluences, the mixing is more evident, but in irregular geometric intersections, it is not apparent with the precision of the previous state. Similarly, Geberemariam [26] concluded that in T and Y shape junctions, the discharge ratio and the area of the separation zone, due to the presence of rotating currents, are inversely related. Generally, it can be said that based on previous studies, various models have been developed and used for pollution transport modeling. Some investigators have simulated the concentration breakthrough curves using statistical distribution models. Another number of them have tried to simulate the mass exchange between the mainstream and the dead zone areas inside the rivers.

Biron et al. conducted numerical simulations of pollutant mixing in an open channel and found that the mixing process was faster when there were inconsistencies in riverbed depths between the main channel and tributaries [6]. The concentration of pollutants in different cross-sectional areas was found to be influenced by the distance from the junction point and the discharge ratio [8].

The flow structure and turbulence at river confluences also play a crucial role in pollutant transport. The shear layer and counter-rotating helical cells in the flow field control the distribution of contaminant concentrations. The turbulent kinetic energy, Reynolds shear stress, and turbulence spectrum are important parameters that affect the turbulent flow structure and the dispersion of

contaminants. The pressure gradient and convective acceleration are key factors in triggering velocity redistribution and influencing the transport of pollutants. However, most of these studies have focused on asymmetrical river confluences, and there is limited research on the transport of contaminants at Y-shaped confluences [27].

Some researchers have also investigated the effect of bedforms on contaminant advection and dispersion [28-31]. Radu et al. [32], using a physical model of a river junction similar to the Danube River, investigated the mixing of pollutants entering the different branches of this river based on a two-dimensional model. In some investigations, including the Tantemsapya et al. [33], an attempt was made to remove or reduce the concentration of pollutants in the river by adding some chemical compounds to the stream. Using a two-dimensional model, Park & Seo [34], investigated contaminant transport through the streams on non-Fickian conditions.

Also, Pengpom et al. [35] performed a two-dimensional numerical finite element simulation through one of Thailand's river confluences. In this research, the impact of flow velocity in the upstream branches and the main channel, as well as the contaminant concentration, were studied. It was concluded that the increasing flow velocity through the upstream branches causes the intense mixing of pollutants and reduced contaminant concentration at the junction.

Lyubimova et al. [36] explored the causes for the weakening of transverse mixing mechanisms through the junctions and claimed that by weakening flow turbulence through the junctions, secondary currents would not appear in this part of the river and consequently, complete mixing flows with different density may not occur even at very long lengths.

Cheng et al. [37] claimed that river confluences significantly impact flow hydraulics, sediment transport, and the size of the riverbed storage area, where a percentage of the pollution mass is temporally trapped. However, it was stated that due to the morphological complexities of river junctions, it is not easy to calculate the contaminant mass trapping rate in the storage area.

From the summary of previous studies, it can be found that many studies have been conducted in the domain of mixing and pollution transport in rivers; however, except for a few cases, many studies have not been done in the area of contaminant mixing through the river junctions. In addition, using two-pulse contaminants injection in the upstream branches will also define more issues of the mixing process through the junction region. Generally, it can be said that a few numbers of analytical equations have been developed regarding the mixing mechanism through the river confluences. For this purpose, the present study was designed to explore more junction zone transport characteristics.

2. Materials and methods

2.1. Experimental data

In order to carry out the present study, a wide laboratory flume was used, and inside it, a Y-shaped junction with different branch widths was created. The laboratory flume had the dimensions of (14x1.2x1) meters in length, width, and height, respectively. The 1.2-meter-wide laboratory flume was divided into two branches with 25 and 45-cm dimensions, intersecting at a 45-degree angle.

The junction was filled with rockfill material with depth of 50 cm to present buried stream junction. A transverse contaminant injector was installed upstream of both branches and was used to employ the mass conservative sodium chloride contaminant solution. The schematic of different parts of the laboratory model of the river junction is depicted in Fig. 1. Four flow discharges of 9, 12, 21, and 25 l/s were employed as flow variables in the experiments, and three initial concentrations of 80, 160, and 200 gr/l were selected and applied as concentration parameters to the upstream branches. Electrical conductivity sensors are installed and connected to the data

logger as depicted in Fig.2. The electrical conductivity recording process started in 2-second intervals. In Fig.2, these sensors' distances and installation conditions are shown in detail through different parts of the experimental model. Sensors No. 1 and 2 were installed in the branch with a width of 45 cm, and sensors No. 3 and 4 were installed in the branch with a width of 25 cm. Sensor No. 5 was used to monitor electrical conductivity variation through the confluence, and finally, sensors No. 6 to 8 were placed downstream of the junction at regular intervals. The experiments were started after stabilizing the flow discharge through the laboratory flume, simultaneously with the injection of the pulse of the pollutant (sodium chloride solution) in both branches. The data recording was also started, and then, by a delay of 15 seconds, the second pulse of the pollutant was injected using a transverse feeder. The sensors recorded the overlap of entrance breakthrough curves. The duration of data collection was controlled through the graphical interface of the data collection system and continued until the concentration recovered to the flume flow's primary concentration.

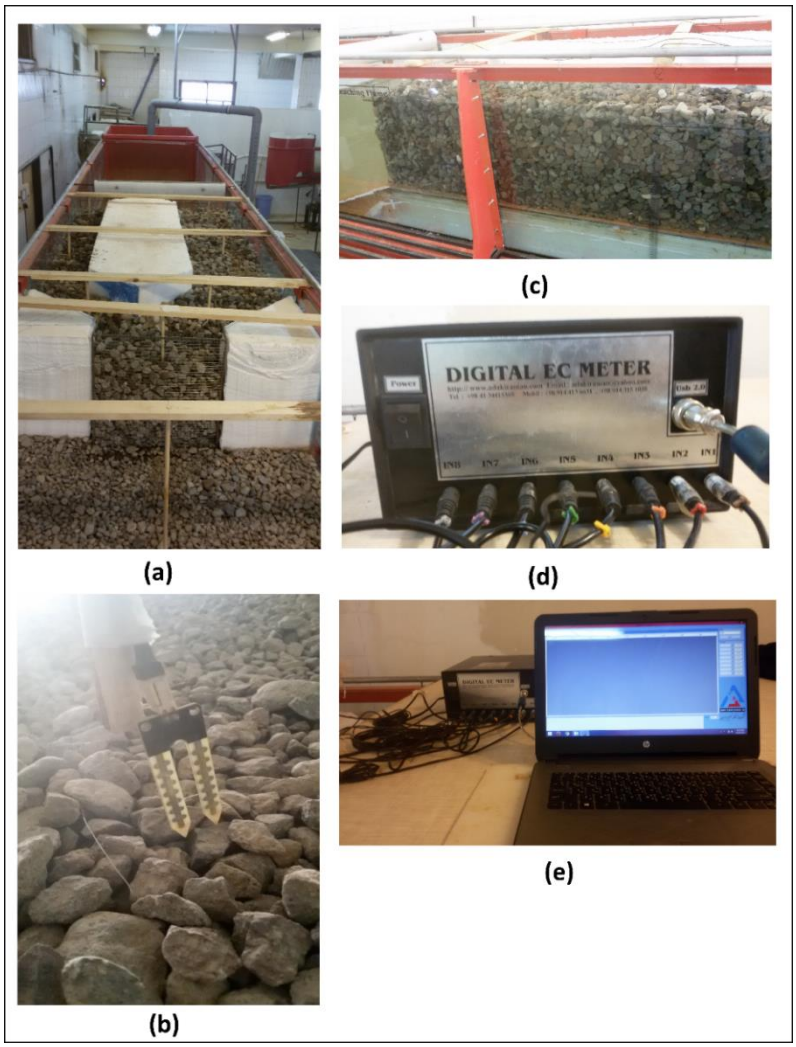

Figure 1. (a) The plan of river laboratory river branches and their junction, (b) installed electrical conductivity sensors (c), filling the area of the river junction to a height of 50 cm (d), data logger of electrical conductivity sensors (e), user interface of data collection software

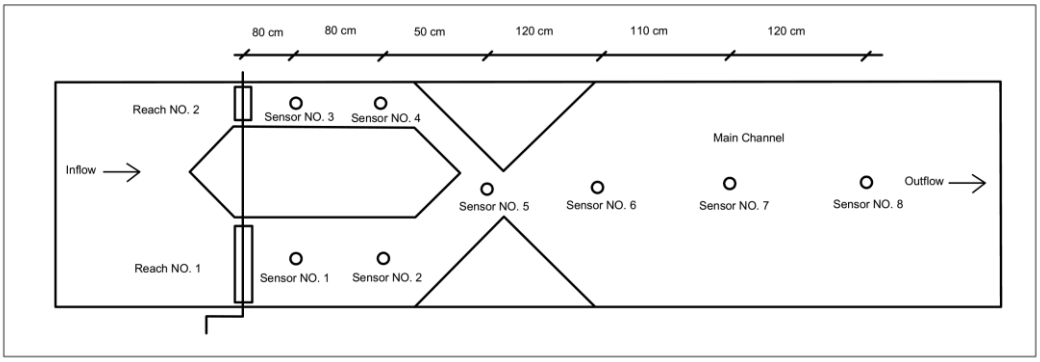

Figure 2. Location of the sensors and their installation distances in the laboratory flume

2.2. Extraction of analytical relationship based on the schematic of pollutant entrance from two upstream branches through the river junction

This research tried to develop a new analytical relationship based on the conceptual model of contaminant entrance from the two upstream branches through the junction by creating a conceptual model and applying the mass conservation relationship. The general method used in extracting this relationship was derived based on the hybrid cell model previously introduced by Ghosh et al. [32]. The general schematic designed cell system for upstream branches and river confluence is shown in Fig. 3. As indicated, the area of the junction is divided into three cells: the first cell represents branch No.1 from the upstream, the second cell represents the branch No. 2 from the upstream, and finally the third cell represents the main river area junction. It also mentions that this relationship is based on completing transverse mixing through the confluence. In other words, the size of this cell is assumed to be large enough so that the complete transverse mixing occurs or the pollution concentration is equal in all parts of this cell. The initial conditions upstream of both cells are expressed as Eqs. 1 and 2.

$$C_1(0) = C_{01}\text{Dirac}(t) \quad (1)$$

$$C_2(0) = C_{02}\text{Dirac}(t) \quad (2)$$

In the above equations, the Dirac(t) function has zero value at all points and infinity at t=0.

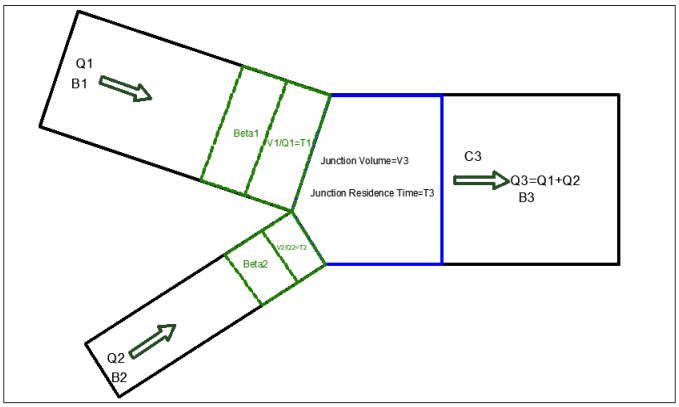

(a)

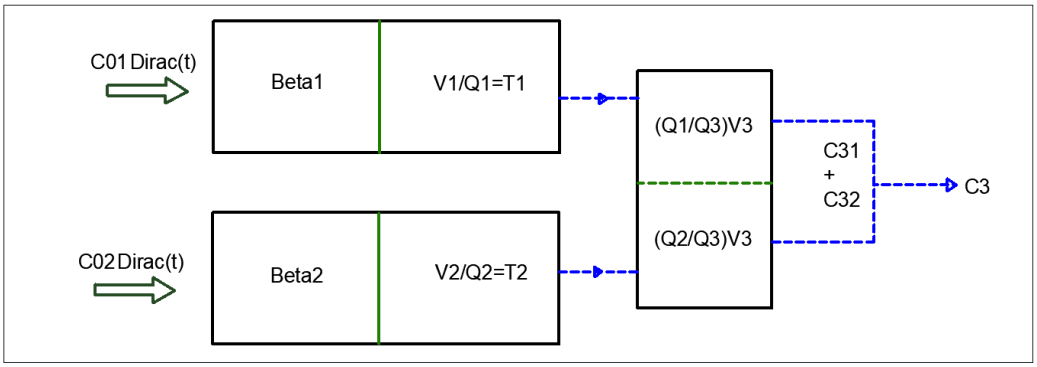

(b)

Figure 3. (a) Cell connections through the river confluence, (b) Schematic of conceptual cells for extracting the analytical relationship

As shown in Fig. 3, the cells of the upstream branches are divided into two separate cells. One is for advection modeling, and the other is for dispersion process modeling of pollutants. The output flow concentration is obtained by applying the upstream initial conditions in the advection cells as Eqs. 4 and 5.

$$C_1(0) = C_{01}\text{Dirac}(t-\beta_1) \quad (3)$$

$$C_2(0) = C_{02}\text{Dirac}(t-\beta_2) \quad (4)$$

The above relationships of β_1 and $\beta_2$equal the residence time of advection cells in the first and second branches upstream of the river junction. Mass conservation equations were written for each cell as the pollutant entered the dispersion cells. The extracted differential equations for the upstream branches of the junction are according to Eqs. 5 and 6.

$$\frac{dC_1(t)}{dt} + C_1(t)\left(\frac{1}{T_1}\right) = \frac{C_{01}\text{Dirac}(t-\beta_1)}{T_1} \quad (5)$$

$$\frac{dC_2(t)}{dt} + C_2(t)\left(\frac{1}{T_2}\right) = \frac{C_{02}\text{Dirac}(t-\beta_2)}{T_2} \quad (6)$$

In the above relationships, T_1 and T_2 are the pollutant residence time through the dispersion cells and are obtained by dividing the cell volume by the flow discharge. For example, $T_1 = \frac{V_1}{Q_1}$, in which V_1 is cell volume, and Q is the passing flow through branch number 1. By assuming the injected pollutant concentration at the beginning of the experiment is equal to C_i, it can be said that the initial condition in the mentioned cells is equal to $C_1(\beta_1) = C_1(\beta_2) = C_i$. Therefore, Eqs. 7 and 8 would be obtained by applying these boundary conditions and solving the above differential equations.

$$C_1(t) = \left(\frac{C_{01}\text{Heaviside}(t-\beta_1)\times\exp\left(\frac{\beta_1}{T_1}\right)}{T_1} + \frac{C_i}{\exp\left(-\frac{\beta_1}{T_1}\right)}\right) \times \exp\left(-\frac{t}{T_1}\right) \quad (7)$$

$$C_2(t) = \left(\frac{C_{02}\text{Heaviside}(t-\beta_2)\times\exp\left(\frac{\beta_2}{T_2}\right)}{T_2} + \frac{C_i}{\exp\left(-\frac{\beta_2}{T_2}\right)}\right) \times \exp\left(-\frac{t}{T_2}\right) \quad (8)$$

In which Heaviside is step function.

By precision in Fig. 3, it is evident that the exiting pollutant from both upstream branches jointly enter a new cell, in which a hypothetical buffer curtain is included. The pollution from upstream branches enters the junction cell. The volume of the junction cell is not divided equally for the entering pollutants from the upstream branches. It was related to the flow rate of each branch. The volume of the mentioned cell is assumed to be equal to V_3, and $Q_3 = Q_1 + Q_2$ is equal to the total discharge of the river main channel, which comes by adding branch discharges. The share of the first branch from the confluence cell is equal to $(\frac{Q_1}{Q_3}) \times V_3$, and similarly the share of the second branch is equal to $(\frac{Q_2}{Q_3}) \times V_3$. Then, the mass conservation equations are written along the confluence cell, and consequently, Eqs. 9 and 10 are obtained.

$$\frac{dC_{31}(t)}{dt} + C_{31}(t)\left(\frac{1}{T_3}\right) = \frac{\left(\frac{C_{01}\text{Heaviside}(t-\beta_1)\times\exp\left(\frac{\beta_1}{T_1}\right)}{T_1} + \frac{C_i}{\exp\left(-\frac{\beta_1}{T_1}\right)}\right)\times\exp\left(-\frac{t}{T_1}\right)}{T_3} \quad (9)$$

$$\frac{dC_{32}(t)}{dt} + C_{32}(t)\left(\frac{1}{T_3}\right) = \frac{\left(\frac{C_{02}\text{Heaviside}(t-\beta_2)\times\exp\left(\frac{\beta_2}{T_2}\right)}{T_2} + \frac{C_i}{\exp\left(-\frac{\beta_2}{T_2}\right)}\right)\times\exp\left(-\frac{t}{T_2}\right)}{T_3} \quad (10)$$

They are solved by applying the initial conditions in the above differential equations as $C_{31}(\beta_1) = C_{32}(\beta_2) = C_i$. The two obtained equations are added together according to the depicted conceptual schematic. In order to further simplify, it is assumed that the initial concentration of the pollutant through the river branches is equal to zero ($C_i = 0$). Ultimately, Eq. 11 is obtained for output contaminant concentration through the confluence.

$$\begin{aligned} C_3(t) = -\frac{1}{(T_1-T_3)(T_2-T_3)}\big((-C_{01}\text{Heaviside}(t-\beta_1)(T_2-T_3)\times \\ \exp\left(\frac{(\beta_1-t)T_3+tT_1}{T_1T_3}\right) - C_{02}\text{Heaviside}(t-\beta_2)(T_1-T_3)\times \\ \exp\left(\frac{(\beta_2-t)T_3+tT_2}{T_2T_3}\right) + C_{01}\text{Heaviside}(t-\beta_1)(T_2-T_3)\times \\ \exp\left(\frac{\beta_1}{T_3}\right) + C_{02}\text{Heaviside}(t-\beta_2)(T_1-T_3)\times\exp\left(\frac{\beta_2}{T_3}\right))\times\exp\left(-\frac{t}{T_3}\right)) \end{aligned} \quad (11)$$

3. Results

3.1. Examining the parameters of the presented analytical model

Pollutant transport in river confluences is influenced by the hydrodynamic characteristics of the flow, including flow velocity, turbulence intensity, and residence time. Experimental modeling helps to understand how these factors affect the movement and spread of pollutants. Studies using experimental modeling have shown that pollutants introduced into the upstream river can be transported along different paths within the confluence zone. Some pollutants are rapidly transported downstream, while others may be trapped within the confluence due to eddies and flow patterns. Additionally, the concentration and distribution of pollutants can vary significantly within the confluence, indicating the complexities of pollutant transport in this dynamic environment.

Considering that the obtained model comes from the combination of inlet breakthrough curves from two upstream branches, it must be capable of reconstructing the double-peak breakthrough curves. Therefore, in the first step, it was tried to investigate this possibility by considering the

numerical values for the model parameters. Fig. 4 is an example of the obtained curves using this model, in which we can see the model's capability.

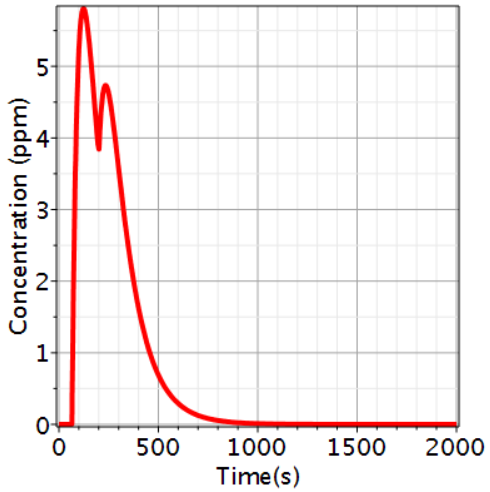

Figure 4. Reconstructing the BC curves by the presented analytical model

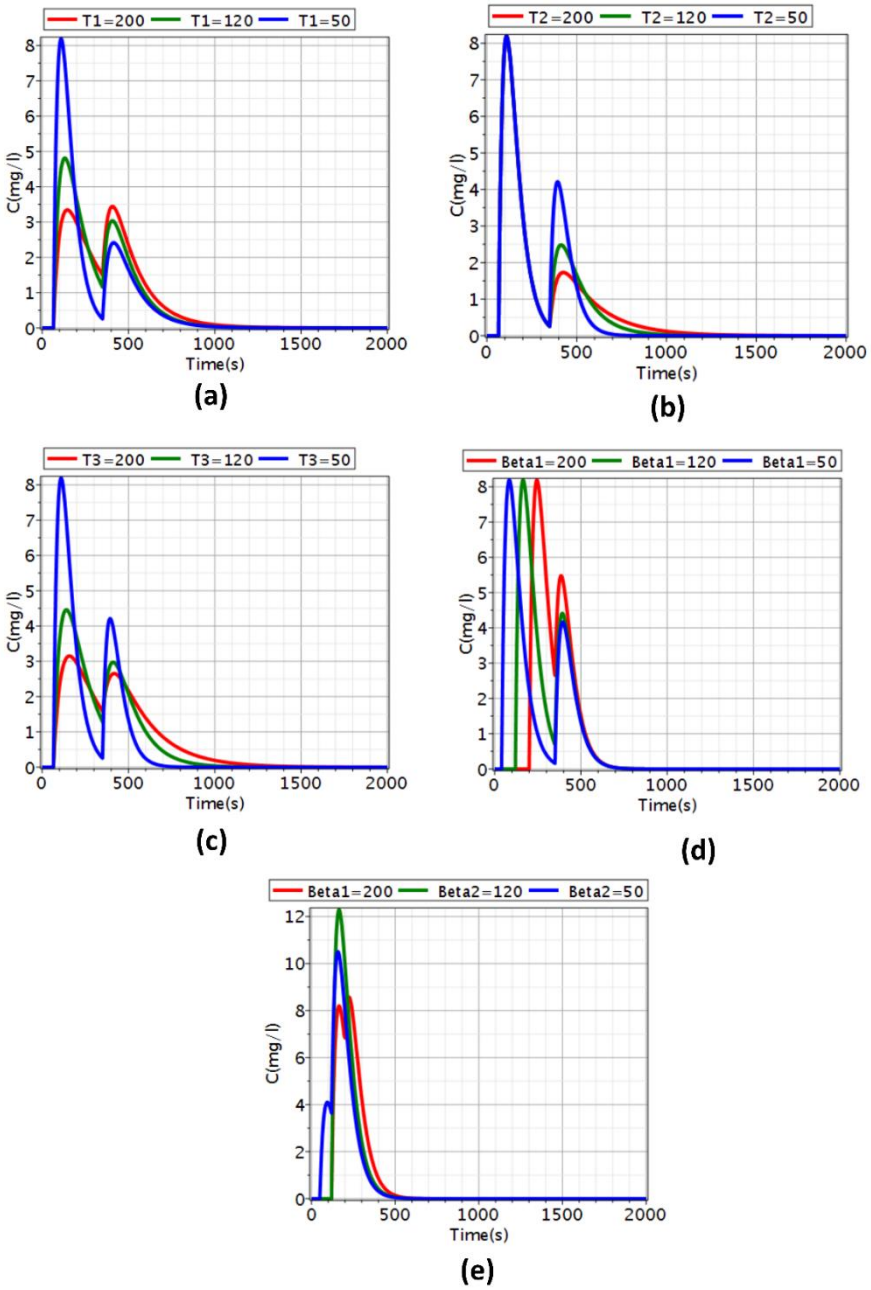

Figure 5. The effect of variation in the model parameters on the shape of the extracted BC curves, (a) the effect of variation in the T_1parameter, (b) the effect of variation in the T_2parameter, (c) the effect of variation in the T_3 parameter, d) the effect of variation in the β_1 parameter, (e) the effect of variation in the β_2 parameter

Then, it was tried to investigate the effect of variation of each parameter in the figure of concentration-time curves. For this purpose, three values of 40, 120, and 200 seconds were used for the model's five temporal parameters, and their effect on the shapes of breakthrough curves was observed. In the first step, by examining the T_1 parameter, it was observed that the increase

of this parameter causes an increase in the spreading power in the first pulse of the breakthrough curve, while in the second pulse, it shows the contrasting effect (Fig. 5, a). The T_2 parameter only affects the second pulse and does not affect the shape of the concentration-time curve in the first pulse (Fig. 5, b). It is worth mentioning that the effect of improving this parameter in the second pulse of the breakthrough curve is similar to T_1 and causes a growth in the pollution spread of the second pulse. The effect of the T_3 parameter is familiar in both pulses of the concentration-time curve, such that with its increase, the dispersion effect is observed in both pulses of the BC curve, and conversely, with its decrease, the maximum concentration values of the curve pulses increase (Figure 5, c). Generally, it can be concluded that the model's temporal parameters are directly related to the dispersion coefficient of the classical advection-dispersion model. However, the effect of these time parameters in the first and second pulses is not the same. Regarding the model's advection time parameters (β_1, β_2), it can be concluded that the β_1 parameter in the first pulse of the curve only has the convection effect, so increasing its value causes shifting of the BC curve toward the right side. However, in the second pulse of the curve, an increase in the maximum concentration is also observed (Fig. 5, d). Otherwise, concerning the β_2 parameter, it can be said that reducing its value causes the second pulse of the curve to merge into the first pulse so that the BC curve's shape transforms from a double peak to a single one (Fig. 5, e).

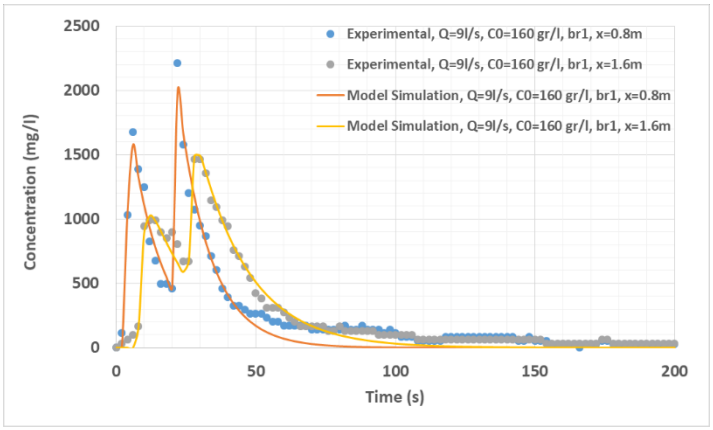

(a)

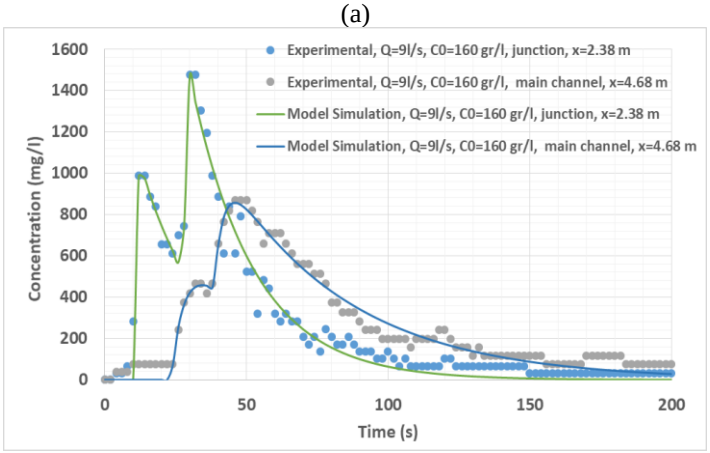

(b)

Figure 6. (a) Observed and simulated BC curves through the upstream branch, (b) Observed and simulated BC curves at the river junction and downstream of the river confluence.

The main issue with the presented analytical model is to examine its simulation capability. For this purpose, the analytical curves were reconstructed and depicted by coding in MATLAB software and extracting the model parameters. Two examples of these simulations are shown in Fig. 6. The first part of this figure is associated with one of the upstream branches, and the second part is related to the junction point and downstream. The general trend shows a good match between the simulated curves and the experimental data. In order to quantitatively evaluate this match, the statistical parameters of root mean square error (RMSE), mean maximum error (MAE), and Nash-Sutcliffe index (DC) were used, and their values were calculated for all the experimental data as 0.1, 72 (ppm) and 0.83, respectively. The Nash-Sutcliffe Efficiency is calculated as one less the error variability of a modeled time series divided by the observed time series variation. Since model errors may have a normal distribution rather than a uniform distribution, RMSE is a good metric for this type of data. In addition, the average absolute error (MAE) measures the average absolute difference between a prediction value and a real value. All errors are given the same weight and are less sensitive to deviations. MAE is useful when it is aimed at minimizing overall errors in the model and avoiding large errors. Computed values also indicate the good performance of the proposed analytical model. It was also observed that by increasing the length and moving downstream of the river confluence, the curves transformed from a two-peaked state to a single-peaked one because of the longitudinal diffusion process.

Further, in order to better understand the advection and dispersion of pollutants in the upstream branches, the junction and the main channel, the process was discussed and investigated using the calculation of the common advection-dispersion parameters. For this purpose, the classical ADE model (Eq. 12) was also used to perform the physical interpretation of this process using ADE model parameters.

$$C(x,t) = \frac{M}{A\sqrt{4\pi Dt}} \exp\left(-\frac{(x-ut)^2}{4Dt}\right) \quad (12)$$

Where M is the injected pollutant mass, A cross section area, D is the longitudinal diffusion coefficient, x is the length parameter, t is the time parameter, and u is the average flow velocity.

For this purpose, after applying the common spatial basis to all the extracted curves, model parameters were also extracted and after depicting them against each other (Fig. 7), their variations were explored. In part (a) of Fig. 7, the longitudinal dispersion coefficient values are plotted versus the distance from the injection site. As is shown, the dispersion coefficient has risen with the increase of the distance parameter, while the scattering of its values has also increased. In part (b), the values of the average velocity are plotted versus the longitudinal dispersion coefficient. It is clear that with the increase of the flow velocity, the dispersion coefficient has also increased. Also in part (c), the values of Peclet number ($P_e = \frac{xu}{D}$), which indicates the ratio of advection power to dispersion in the river channel, are plotted versus the values of diffusivity ($\frac{D}{u}$). As indicated, the transmisability values have decreased exponentially with the increase of Peclet number, and finally, in part (d) of Fig. 7, the variation of Peclet number are plotted against the longitudinal distance from the injection site. It was observed that Pe numbers increase with the growth of the length parameter, which indicates that the transfer process is stronger than the dispersion process.

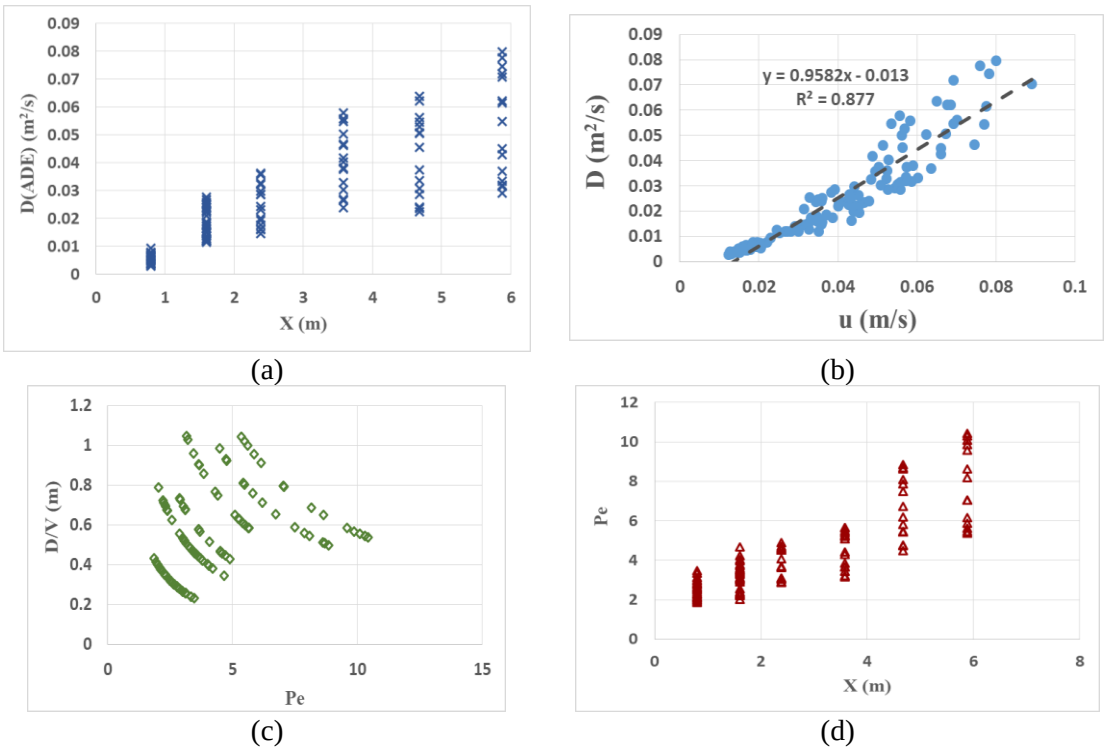

Figure 7. (a) D parameter variation along the river, (b) D parameter versus u parameter, (c) D/u parameter variation versus Peclet number, (d) Peclet number variations versus distance

4. Conclusion

In the quantitative investigation of the advection and dispersion process of pollutants through the river network, their detailed analysis at river junctions is one of the most critical issues. Due to the lack of knowledge in this regard, in the current study, it was tried to create a conceptual model of a river confluence with two sub-branches. Then, solving differential equations, an explicit equation was extracted based on the cell residence time characteristics of the upstream branches and junction zone. The presented relationship can create two-part and double-peak curves according to the general nature of the breakthrough curves through the confluences. Sodium chloride solution was selected as a mass conservative pollutant, and laboratory data was acquired. The results showed a very good agreement with the analytical model. All model parameters are temporal and gain different values based on residence time through the different parts of the conceptual model. In order to examine the temporal parameter's effect, they were varied one by one by keeping the rest of the parameter's constant, and then the artificial concentration-time curves were produced and analyzed. Additionally, the analytical curves were reconstructed and depicted by coding in MATLAB software and extracting the model parameters. The general trend shows a good match between the simulated curves and the experimental data. The model's temporal parameters were also extracted and after depicting them against each other, their variations were explored. The results show that the dispersion coefficient has risen with the increase of the distance parameter, while the scattering of its values has also increased. It was also observed that the Pe numbers increase with the growth of the length parameter, which indicates that the transfer process is stronger than the dispersed process. Generally, it was observed that the increase in the residence time of the pollutant through the diffusion cells of the model (T) causes

an increase in dispersion. On the other hand, an increase in the model's advection parameter (β) causes the right side shifting of the curve. Next, applying the least squares curve fitting method to the collected laboratory data, the actual model parameters were estimated, and then theoretical curves were created versus experimental ones. Three statistical parameters (RMSE), (MAE), and (DC) were used to test the efficiency of the model. The values of these three parameters were equal to 0.1, 72 (ppm), and 0.83, respectively, which indicates the proper functioning of the presented analytical model.

References

1. J. Chabokpour, B. Chaplot, M. Dasineh, A. Ghaderi, and H. M. Azamathulla, "Functioning of the multilinear lag-cascade flood routing model as a means of transporting pollutants in the river," *Water Supply*, vol. 20, no. 7, pp. 2845-2857, 2020.
2. J. Chabokpour, H. M. Azamathulla, Y. Azhdan, and M. Ziaei, "Study of pollution transport through the river confluences by derivation of an analytical model," *Water Science and Technology*, vol. 82, no. 10, pp. 2062-2075, 2020.
3. J. L. Best, "Flow dynamics and sediment transport at river channel confluences," Birkbeck (University of London), 1985.
4. J. L. Best, "Flow dynamics at river channel confluences: implications for sediment transport and bed morphology," 1987.
5. J. L. Best, "Sediment transport and bed morphology at river channel confluences," *Sedimentology*, vol. 35, no. 3, pp. 481-498, 1988.
6. P. Biron, J. L. Best, and A. G. Roy, "Effects of bed discordance on flow dynamics at open channel confluences," *Journal of Hydraulic Engineering*, vol. 122, no. 12, pp. 676-682, 1996.
7. J. L. Best and I. Reid, "Separation zone at open-channel junctions," *Journal of Hydraulic Engineering*, vol. 110, no. 11, pp. 1588-1594, 1984.
8. J. Chabokpour and A. Samadi, "Analytical solution of reactive hybrid cells in series (HCIS) model for pollution transport through the rivers," *Hydrological Sciences Journal*, vol. 65, no. 14, pp. 2499-2507, 2020.
9. J. Chabokpour, "Study of pollution transport through the rivers using aggregated dead zone and hybrid cells in series models," *International Journal of Environmental Science and Technology*, vol. 17, no. 10, pp. 4313-4330, 2020.
10. Y. Qing-Yuan, W. Xian-Ye, L. Wei-Zhen, and W. Xie-Kang, "Experimental study on characteristics of separation zone in confluence zones in rivers," *Journal of Hydrologic Engineering*, vol. 14, no. 2, pp. 166-171, 2009.
11. M. Leite Ribeiro, K. Blanckaert, A. Roy, and A. J. Schleiss, "Flow and sediment dynamics in channel confluences," *Journal of Geophysical Research: Earth Surface*, vol. 117, no. F1, 2012.
12. P. Biron, B. De Serres, A. Roy, and J. L. Best, "Shear layer turbulence at an unequal depth channel confluence," in *Turbulence: Perspectives on Flow and Sediment Transfer*: John Wiley & Sons, Ltd., 1993, pp. 197-213.
13. B. L. Rhoads and A. N. Sukhodolov, "Spatial and temporal structure of shear layer turbulence at a stream confluence," *Water Resources Research*, vol. 40, no. 6, 2004.
14. A. Shakibainia, M. R. M. Tabatabai, and A. R. Zarrati, "Three-dimensional numerical study of flow structure in channel confluences," *Canadian Journal of Civil Engineering*, vol. 37, no. 5, pp. 772-781, 2010.

15. S. Yuan, H. Tang, Y. Xiao, X. Qiu, H. Zhang, and D. Yu, "Turbulent flow structure at a 90-degree open channel confluence: Accounting for the distortion of the shear layer," *Journal of hydro-environment research*, vol. 12, pp. 130-147, 2016.
16. B. De Serres, A. G. Roy, P. M. Biron, and J. L. Best, "Three-dimensional structure of flow at a confluence of river channels with discordant beds," *Geomorphology*, vol. 26, no. 4, pp. 313-335, 1999.
17. K. Bradbrook, S. Lane, K. Richards, P. Biron, and A. Roy, "Role of bed discordance at asymmetrical river confluences," *Journal of hydraulic engineering*, vol. 127, no. 5, pp. 351-368, 2001.
18. X.-g. Wang, Z.-m. Yan, and W.-d. Guo, "Three-dimensional simulation for effects of bed discordance on flow dynamics at Y-shaped open channel confluences," *Journal of Hydrodynamics, Ser. B*, vol. 19, no. 5, pp. 587-593, 2007.
19. C. Boyer, A. G. Roy, and J. L. Best, "Dynamics of a river channel confluence with discordant beds: Flow turbulence, bed load sediment transport, and bed morphology," *Journal of Geophysical Research: Earth Surface*, vol. 111, no. F4, 2006.
20. G. H. Jirka, *Mixing and dispersion in rivers*. Taylor and Francis, London, 2004.
21. J. M. Gaudet and A. G. Roy, "Effect of bed morphology on flow mixing length at river confluences," *Nature*, vol. 373, no. 6510, pp. 138-139, 1995.
22. E. Mignot, I. Vinkovic, D. Doppler, and N. Riviere, "Mixing layer in open-channel junction flows," *Environmental Fluid Mechanics*, vol. 14, pp. 1027-1041, 2014.
23. G. Weidong and W. X. J. T. Yue, "Research of Hydraulic Characteristics of "Y" shaped Junction," *Hydroelectric Energy*, 2005.
24. G. Weidong, W. Xiaogang, Y. Jiwen, Y. Tianen, and L. Yue, "Research of Hydraulic Characteristics of "Y" shaped Junction," *Water Resour. Power*, vol. 23, pp. 53-56, 2005.
25. B. L. Rhoads and A. N. Sukhodolov, "Field investigation of three-dimensional flow structure at stream confluences: 1. Thermal mixing and time-averaged velocities," *Water resources research*, vol. 37, no. 9, pp. 2393-2410, 2001.
26. T. K. Geberemariam, "Numerical analysis of stormwater flow conditions and separation zone at open-channel junctions," *Journal of Irrigation and Drainage Engineering*, vol. 143, no. 1, p. 05016009, 2017.
27. J. Chabokpour and H. M. Azamathulla, "Numerical simulation of pollution transport and hydrodynamic characteristics through the river confluence using FLOW 3D," *Water Supply*, vol. 22, no. 10, pp. 7821-7832, 2022.
28. K. E. Bencala, "Simulation of solute transport in a mountain pool-and-riffle stream with a kinetic mass transfer model for sorption," *Water Resources Research*, vol. 19, no. 3, pp. 732-738, 1983.
29. A. Marion, M. Zaramella, and A. Bottacin-Busolin, "Solute transport in rivers with multiple storage zones: The STIR model," *Water resources research*, vol. 44, no. 10, 2008.
30. A. Bottacin-Busolin and A. Marion, "Combined role of advective pumping and mechanical dispersion on time scales of bed form–induced hyporheic exchange," *Water Resources Research*, vol. 46, no. 8, 2010.
31. X. Chen, M. B. Cardenas, and L. Chen, "Hyporheic exchange driven by three-dimensional sandy bed forms: Sensitivity to and prediction from bed form geometry," *Water Resources Research*, vol. 54, no. 6, pp. 4131-4149, 2018.
32. V. M. Radu, E. Diacu, M. A. Moncea, F. D. Dumitru, A. M. Panait, and P. Ionescu, "Numerical modelling of pollutant dispersion in the lower Danube River," *Rev Chim Bucharest*, vol. 68, no. 11, pp. 2477-2481, 2017.

33. N. Tantemsapya, W. Wirojanagud, and S. Suwannakom, "Modeling approach to water quality management in the lower Pong river, Thailand," *Warasan Wichai Mokho,* 2008.
34. I. Park and I. W. Seo, "Modeling non-Fickian pollutant mixing in open channel flows using two-dimensional particle dispersion model," *Advances in water resources,* vol. 111, pp. 105-120, 2018.
35. N. Pengpom, S. Vongpradubchai, and P. Rattanadecho, "Numerical Analysis of Pollutant Concentration Dispersion and Convective Flow in a Twodimensional Confluent River Model," *Mathematical Modelling of Engineering Problems,* vol. 6, no. 2, 2019.
36. T. Lyubimova, A. Lepikhin, Y. N. Parshakova, C. Gualtieri, S. Lane, and B. Roux, "Influence of hydrodynamic regimes on mixing of waters of confluent rivers," *Journal of Applied Mechanics and Technical Physics*, vol. 60, pp. 1220-1227, 2019.
37. D. Cheng, J. Song, W. Wang, and G. Zhang, "Influences of riverbed morphology on patterns and magnitudes of hyporheic water exchange within a natural river confluence," *Journal of hydrology*, vol. 574, pp. 75-84, 2019.